Journal of Porous Media, 17 (11): 937–952 (2014)

COMPOSITIONAL EFFECTS IN LIGHT/MEDIUM OIL RECOVERY BY AIR INJECTION: VAPORIZATION VS. COMBUSTION

Negar Khoshnevis Gargar,[1,*] Alexei A. Mailybaev,[2] Dan Marchesin,[2] & Hans Bruining[1]

[1]*Delft University of Technology, Civil Engineering and Geosciences, Stevinweg 1, 2628 CE Delft, The Netherlands*

[2]*Instituto Nacional de Matemática Pura e Aplicada (IMPA), Estrada Dona Castorina 110, Rio de Janeiro 22460-320, Brazil*

[*]Address all correspondence to Negar Khoshnevis Gargar E-mail: N.khoshnevisgargar@tudelft.nl

Original Manuscript Submitted: 1/7/2014; Final Draft Received: 8/5/2014

Combustion can be used to enhance recovery of heavy, medium, or light oil in highly heterogeneous reservoirs. Such broad range of applicability is attained because not only do the high temperatures increase the mobility of viscous oils but also the high thermal diffusion spreads the heat evenly and reduces heterogeneity effects. For the latter reason, combustion is also used for the recovery of light oils. The reaction mechanisms are different for light oils, where vaporization is dominant, whereas for medium nonvolatile oils combustion is dominant. We will only consider combustion of medium and light oils. Therefore we ignore coke formation and coke combustion. It is our goal to investigate the relative importance of vaporization and combustion in a two-component mixture of volatile and nonvolatile oils in a low air injection rate regime. By changing the composition we can continuously change the character of the combustion process. We derive a simplified model for the vaporization/combustion process, and implement it in a finite element package, COMSOL. For light oil mixtures, the solution consists of a thermal wave upstream, a combined vaporization/combustion wave in the middle (with vaporization upstream of combustion) and a saturation wave downstream. For medium mixtures the vaporization/condensation sequence is reversed and vaporization moves ahead of the combustion. Due to its low viscosity, the light oil is displaced by the gases to a region outside the reach of oxygen and therefore less oil remains behind to reach the combustion zone. This leads to a high combustion front velocity. For oil with more nonvolatile components, vaporization occurs downstream of the combustion zone. As more oil stays behind to feed the combustion zone, the velocity of the combustion zone is slower, albeit the temperatures are much higher. The relative importance of vaporization/combustion depends also on the injection rate, pressure, initial temperature, and oil viscosity. Numerical calculations allow to estimate the bifurcation points where the character of the combustion changes from a vaporization-dominated to a combustion-dominated process.

KEY WORDS: *in situ combustion, vaporization, medium temperature oxidation, light oil recovery, air injection*

1. INTRODUCTION

In situ combustion is generally considered as a technique that is applicable to heavy oils because of the significant reduction in oil viscosity. However, it also promotes production through thermal expansion, distillation, and gas drive generated by the combustion gases, so it can also be used to recover light oils. In this case the air injection process is often referred to as "high pressure air injection" and can be applied to deep light oil reservoirs,

1091–028X/14/$35.00

NOMENCLATURE

A_{rl}	light oil MTO reaction preexponential factor (1/s)
A_{rm}	medium oil MTO reaction preexponential factor (1/s)
C_o, C_g	heat capacity of oil and gas [J/(mol·K)]
C_m	heat capacity of porous matrix [J/(m^3·K)]
D_o	oil diffusion coefficient (m^2/s)
D_g	gas diffusion coefficient (m^2/s)
k_o, k_g	oil and gas phase permeabilities (m^2)
k_{ro}, k_{rg}	oil and gas phase relative permeabilities
n	MTO reaction order with respect to oxygen
P_g	prevailing gas pressure (Pa)
P_o	prevailing oil pressure (Pa)
Q_{rl}	light oil MTO reaction enthalpy per mole of oxygen (J/mol)
Q_{rm}	medium oil MTO reaction enthalpy per mole of oxygen (J/mol)
Q_v	liquid fuel vaporization heat at reservoir temperature (J/mol)
R	ideal gas constant [J/(mol·K)]
s_o, s_g	saturations of oil and gas phases
t	time (s)
T	temperature (K)
T^{bl}	boiling temperature of light component (K)
T^{ini}	reservoir temperature (K)
T_l^{ac}	light oil MTO activation temperature (K)
T_m^{ac}	medium oil MTO activation temperature (K)
u_o, u_g, u	oil, gas, and total Darcy velocities (m/s)
u_{gj}	Darcy velocity of gas components $j = l, \kappa, r$ (hydrocarbon, oxygen, rest) (m/s)
u_{oi}	Darcy velocity of component $i = l, m$ (light, medium) in oil phase (m/s)
u^{inj}	injection Darcy velocity of gas (m/s)
W_v, W_{rl}, W_{rm}	vaporization rate, light oil, and medium oil MTO reaction rates [mol/(m^3·s)]
x	spatial coordinate (m)
X_l, X_m	oil molar fractions: light and medium components (mol/mol)
Y_l, Y_κ, Y_r	gas molar fractions: hydrocarbons, oxygen, remaining components (mol/mol)
Y_κ^{inj}	oxygen fraction in injected gas

Greek Symbols

λ	thermal conductivity of porous medium [W/(m·K)]
μ_o, μ_g	viscosity of oil and gas (Pa·s)
$\nu_{ol}, \nu_{gl}, \nu_{om}, \nu_{gm}$	stoichiometric coefficients in the MTO reactions
ρ_o, ρ_g	molar densities of oil and gas (mol/m^3)
ρ_{gl}, ρ_κ, ρ_r	molar densities of hydrocarbon, oxygen, and remaining in gas phase (mol/m^3)
ρ_{ol}, ρ_{om}	molar densities of light and medium hydrocarbon in oil phase (mol/m^3)
ρ_L, ρ_M	pure phase densities of light and medium hydrocarbon in oil phase (mol/m^3)
φ	porosity
ψ_l, ψ_m	volume fractions in oleic phase: light and medium components (m^3/m^3)

whereas the term "in situ combustion" (ISC) traditionally has been used for heavy oil reservoirs. Our interest is in recovering relatively low viscosity oil from low permeability heterogeneous reservoirs using air injection leading to oil combustion. Therefore, we will consider combustion of medium and light oils rather than of heavy oils. Air injection can be effective in heterogeneous permeability reservoirs as the oil evaporates away from the lower permeability parts to be collected in the higher mobility streaks. High solubility of the light components in liquid fuel is an advantage of high pressures, leading to a higher oil recovery (Mailybaev et al., 2013).

There is a large body of literature describing the use of HPAI (high pressure air injection, starting at ∼100 bars) to recover oil. There are technically and economically successful HPAI projects applied in light oil reservoirs (Fassihi et al., 1997; Huffman et al., 1983; Parrish et al., 1974a,b). Application of HPAI is confined to reservoirs at large depths, because high pressures need to be applied. However, at shallower depths, an alternative is to inject at medium pressures (∼10–90 bars) for light and medium oil in heterogeneous low permeability reservoirs. The question is whether acceptable recovery efficiencies can also be obtained at medium pressures. We will show

that combustion process at medium pressures is characterized by medium temperature oxidation (MTO) wave. In this wave all physical processes, reaction, vaporization, condensation, and filtration are active. The name of the wave comes from the fact that the maximum temperature is bounded by liquid boiling temperature at elevated pressure and, thus, cannot be very high. De Zwart et al. (2008) compare equation of state (EOS) models with multicomponent combustion models to assess their applicability to in situ combustion under HPAI conditions. Even for HPAI, De Zwart et al. conclude that air injection cannot be modeled as a flue gas displacement process as this leads to an underestimate of the recovery, because certain thermal aspects are not adequately captured (Montes et al., 2010), such as stripping and condensation mechanisms. It is also concluded by Montes et al. (2010) that HPAI is more than a simple gas flood. Some of the residual oil can be moved and mobilized by the thermal processes; this "extra oil" can be driven towards the production wells either by the flue-gas drive or thermal processes. In other words, these thermal processes play an important role also at medium pressures; these are the focus of this paper.

Combustion of light oil and medium oil (Abou-Kassem et al., 1986; Akin et al., 2000; Bruining et al., 2009; Castanier and Brigham, 1997, 2003; Kok and Karacan, 2000; Lin et al., 1984, 1987; Mailybaev et al., 2011a; Wahle et al., 2003; Xu et al., 2004) are described by different mechanisms. Indeed, the mechanism actually responsible for oil displacement in the combustion process varies with the type of oil. For medium viscosity oils with medium boiling points, the oxygen in the air burns heavier components of the oil, generating heat leading to coking, cracking, and vaporization of lighter components, in which lighter components move out of the reach of oxygen. For light oil, the small amount of coke formation is usually disregarded, although it can occur (Khoshnevis Gargar et al., 2010). Also, vaporization and condensation are equally important as the oxidation reaction (Mailybaev et al., 2013). As opposed to medium oil combustion, light oil combustion usually occurs at lower temperatures, because vaporization displaces part of the fluid out of reach of the combustion process and consequently the fuel concentration in the combustion zone becomes low. However, when little vaporization occurs, a larger part of the oil is oxidized and relatively high temperatures can still occur, which is a result obtained in this paper.

At low temperatures, the crude oil can undergo oxidation reactions with or without small amounts of carbon monoxide and dioxide generation. Rather, oxygenated hydrocarbons are formed. This is usually termed "low temperature oxidation" (LTO). As the temperature rises, distillation coupled with pyrolysis produces hydrogen gas and some light hydrocarbons in the gas phase. A major part of light hydrocarbons is produced as they move outside the reach of oxygen (Fassihi et al., 1984). However, oxygen reacts with light hydrocarbons left behind and therefore medium temperature oxidation (MTO) occurs, which produces, e.g., CO and CO_2. Further increase of the temperature leads to deposition and combustion of coke, and the combustion process is called HTO. When coke concentration is sufficient for complete consumption of air, the hydrocarbon ahead of the combustion front does not contact oxygen. In contrast, in the case of low fuel concentration a significant amount of oxygen moves ahead of the combustion zone (Mailybaev et al., 2011a,b). This results in an LTO process downstream. The viscosity of oxygenated crude oil is higher than the viscosity of the original crude (Poling et al., 2001). The activation energy for LTO is generally lower than that for HTO (Kumar et al., 2010).

In summary, we have high temperature oxidation (HTO), when cracking occurs and coke is formed, which is subsequently oxidized at high temperatures; low temperature oxidation (LTO), when the oxygen is incorporated in the hydrocarbon molecules to form alcohols, aldehydes, acids, or other oxygenated hydrocarbons (Greaves et al., 2000a,b; Hardy et al., 1972); and medium temperature oxidation (MTO) (Germain and Geyelin, 1997; Greaves et al., 2000b; Gutierrez et al., 2009), when the oxidation reaction leads to scission of the molecules and to the formation of small reaction products such as water, CO, or CO_2. It is the purpose of this paper to quantify the relative importance of vaporization/condensation and oxidation for light oil in an MTO process, and relate it to the oil composition, air injection rate, and pressure. We propose a simplified model considering light oil recovery through displacement by air at medium pressures. The presence of liquid fuel, which is mobile and can vaporize or condense, is a challenge for modeling the combustion process. We only consider the one-dimensional flow problem, expecting that its solution contributes to the understanding of the MTO process (Germain and Geyelin, 1997; Greaves et al., 2000b; Gutierrez et al., 2009).

A number of conceptual combustion models describing ISC have been studied theoretically and experimentally in the past (Abou-Kassem et al., 1986; Akin et al., 2000; Akkutlu et al., 2004, 2005; Alexander et al., 1962; Belgrave and Moore, 1992; Bruining et al., 2009; Castanier and Brigham, 1997, 2003; Fassihi et al., 1984; Kok

and Karacan, 2000; Lin et al., 1984, 1987; Xu et al., 2004; Yortsos and Akkutlu, 2001). Most of the models assume liquid phase or coke combustion as the source of energy to sustain ISC and high temperature oxidation. There are also papers that focus on numerical simulation of the combustion process (Adegbesan et al., 1987; Crookston et al., 1979; Gerritsen et al., 2004; Gottfried et al., 1965; Khorsandi Kouhanestani et al., 2011; Kumar et al., 1987; Lin et al., 1984; Youngren et al., 1980). These papers deal with the kinetics of the reactions for light and heavy oil (Lin et al., 1984), fluid phase behavior, heat losses and different numerical schemes. Khorsandi Kouhanestani et al. (2011) focus on the complex phase behavior. Medium pressure air injection has been studied less extensively. The combustion of light oil at medium pressure (10–90 bars) is introduced as medium temperature oxidation (MTO) in this paper, as the temperature is controlled by evaporation. Greaves et al. (2000b) carried out two tests on a light Australian oil (38.8° API) starting at initial oil saturations of S_o = 0.41 and 0.45, at an operating pressure of 70 bard and an initial bed temperature of 63°C. The combustion temperature was about 250°C in both tests. Gillham et al. (1998) show that for the deep Hackberry reservoir, air injection can increase the light oil recovery to economical significance. They distinguish between application of high and low pressures in the field trials. The low pressure trial is conducted between 20 and 40 bars. Unfortunately, supporting tube tests were only reported at high pressures (230 bars). The paper reports two incidents of fire, one in the high pressure test and one in the low pressure test, both occurring in the injection well. Gutierrez et al. (2008) describe a low pressure (14 bars) laboratory test with light oil, which gave rise to relatively high temperatures (478°C). Khoshnevis Gargar et al. (2014b) carried out air injection experiments with one-component oil at medium pressures and low injection rate, they found out that physical and chemical sorption of oxygen occurs at low temperatures before the scission reaction. Germain and Geyelin (1997) describe combustion tube tests with light oil in heterogeneous low permeability (1–100 mD) reservoirs using pressures of 40–45 bars and leading to combustion temperatures between 260°C and 370°C. Low pressure thermal gravity and differential scanning calorimetry test results (Li et al., 2004) show that distillation is the dominant process for the recovery of light and medium oils at elevated temperatures. The process studied in this paper is very similar to the mechanism described here.

Because the MTO process has been studied only in models with one hydrocarbon pseudo-component (Mailybaev et al., 2013), we assert that our understanding of the oxidation/vaporization/condensation mechanisms in MTO wave can be improved by considering a simple model involving a two-component oil mixture, e.g., heptane and decane in dry porous rock. Heptane and decane represent pseudo-components as volatile and nonvolatile components respectively, which are characterized by an average boiling temperature, density, and viscosity for each. Heptane represents the light component, which can both evaporate and combust, whereas decane represents the medium fraction of the mixed oil, which we assume to react with oxygen, but it cannot vaporize. The main discerning factor in the MTO combustion process is the ratio between vaporization, and combustion in the low injection rate regime. It turns out that the oxidation, vaporization and condensation often occur close to each other in the MTO wave in the case of the larger presence of light components. Vaporization occurs upstream of the combustion zone. The temperature variation is bounded by the oil boiling temperature. Such regime is in good agreement with the predictions based on a single pseudo-component model (Mailybaev et al., 2013). We show that adding more non volatile components reverts the sequence of oxidation/vaporization in the MTO wave. This leads to much higher temperatures, eventually changing the combustion regime to HTO. The overall flow consists of three waves, viz., the thermal, MTO, and saturation wave.

The paper is organized as follows. Section 2 describes the physical model and presents the governing equations. Section 3 describes analytical solutions and the MTO wave profile for an oil model with one pseudo-component. Section 4 presents numerical solutions of the two-component model for several sets of conditions. We end with some conclusions.

2. MODEL

We study a two-phase flow problem including combustion when air is injected into porous rock filled with oil composed of light and medium fractions. The light oil (volatile component) can both evaporate and oxidize, whereas the medium oil (non volatile component) can only oxidize. In our applications, we disregard gas-phase reactions, while it is still a matter of debate whether gas-phase reactions play a significant role in porous media as annihilation of free radicals at the pore walls will drastically reduce the reaction rates (Bamford and Tipper, 1977; Fisher et al., 2000; Helfferich, 2004; Levenspiel, 1999; Schott, 1960). We can summarize the reaction process in the following reaction equations:

$$\begin{aligned}&\nu_{ol}\ \text{light hydrocarbons} + O_2 \rightarrow \nu_{gl}\ \text{gaseous products},\\ &\nu_{om}\ \text{medium hydrocarbons} + O_2 \rightarrow \nu_{gm}\ \text{gaseous products},\end{aligned} \tag{2.1}$$

i.e., one mole of oxygen reacts with ν_{oi} moles of oleic (liquid) hydrocarbons ($i = l$, light and $i = m$, medium fractions) generating ν_{gi} moles of gaseous products (H_2O, CO_2, etc.). This system is studied in 1D, allowing for the presence of oil and gas. The liquid oil saturation is s_o and the gas saturation is $s_g = 1 - s_o$. In the gaseous phase, we distinguish between the molar fraction of hydrocarbon gas Y_l and the molar fraction of oxygen Y_κ. The medium oil component does not exist in the gaseous phase. The remaining components with molar fraction $Y_r = 1 - Y_\kappa - Y_l$ consist of reaction products and inert components of the injected gas. X_m and X_l are the mole fractions of the medium (non volatile) and light (volatile) components in the oleic phase ($X_m + X_l = 1$).

In the model that follows we will assume that the light oil and medium oil behave as an ideal mixture with neither heat nor volume effects due to mixing. Then the oil density can be expressed as $\rho_o = \psi_m \rho_M + \psi_l \rho_L$, where ψ_m and ψ_l are the volume fractions of the medium and light components ($\psi_m + \psi_l = 1$), and ρ_M and ρ_L are the pure oleic densities of the medium and light components, respectively. The volume and molar fractions are related by

$$\rho_{om} = X_m \rho_o = \psi_m \rho_M, \quad \rho_{ol} = X_l \rho_o = \psi_l \rho_L, \tag{2.2}$$

where ρ_{om} and ρ_{ol} are molar densities of medium and light components in the oleic phase. For the ideal gas, the molar and volume fractions coincide. The molar densities of gas components are given by $\rho_{gl} = Y_l \rho_g$, $\rho_\kappa = Y_\kappa \rho_g$ and $\rho_r = Y_r \rho_g$.

The molar mass balance equations for liquid and gas components can be written as

$$\partial_t(\varphi \rho_{om} s_o) + \partial_x(\rho_M u_{om}) = -\nu_{om} W_{rm}, \tag{2.3}$$

$$\partial_t(\varphi \rho_{ol} s_o) + \partial_x(\rho_L u_{ol}) = -\nu_{ol} W_{rl} - W_v, \tag{2.4}$$

$$\partial_t(\varphi \rho_{gl} s_g) + \partial_x(\rho_g u_{gl}) = W_v, \tag{2.5}$$

$$\partial_t(\varphi \rho_\kappa s_g) + \partial_x(\rho_g u_{g\kappa}) = -W_{rm} - W_{rl}, \tag{2.6}$$

$$\partial_t(\rho_r s_g) + \partial_x(\rho_g u_{gr}) = \nu_{gm} W_{rm} + \nu_{gl} W_{rl}, \tag{2.7}$$

where $u_{\alpha j}$ means the Darcy velocity of component j in phase α. In summary, there are four components, viz., light oil (l), medium oil (m), oxygen (κ), and the rest (r). The light component can exist in the oleic phase (o) and the gaseous phase (g), the medium component only exists in the oleic phase (o), whereas oxygen and the remaining gases can only exist in the gaseous phase.

The oleic, gaseous phase, and total Darcy velocities are

$$u_o = -\frac{k_o}{\mu_o}\frac{\partial P_o}{\partial x}, \quad u_g = -\frac{k_g}{\mu_g}\frac{\partial P_g}{\partial x}, \quad u = u_g + u_o. \tag{2.8}$$

In this equation $\mu_o(T, X_m)$ and $\mu_g(T)$ are the oleic and gaseous phase viscosities. For the gas viscosity μ_g composition dependency is disregarded. P_o is the oleic phase pressure and P_g is the gaseous phase pressure. We disregard capillary forces in what follows; i.e., we take $P_o = P_g$. We denote the permeability of phase α by k_α. We use the ideal gas law to relate the molar density ρ_g to the pressure P_g,

$$\rho_g = \frac{P_g}{RT}. \tag{2.9}$$

One can derive the following expressions for the velocity of the medium and light components in the oleic phase as (Bird et al., 2002)

$$\begin{aligned}u_{om} &= \psi_m u_o - \varphi s_o D_o \partial_x \psi_m,\\ u_{ol} &= \psi_l u_o - \varphi s_o D_o \partial_x \psi_l,\end{aligned} \tag{2.10}$$

where D_o is the oleic liquid diffusion coefficient, which we take as $D_o = 10^{-10}$ m^2/s. Similarly we approximate the velocities of the components in the gas phase by

$$\begin{aligned}u_{gl} &= Y_l u_g - \varphi s_g D_g \partial_x Y_l,\\ u_{g\kappa} &= Y_\kappa u_g - \varphi s_g D_g \partial_x Y_\kappa,\\ u_{gr} &= Y_r u_g - \varphi s_g D_g \partial_x Y_r.\end{aligned} \tag{2.11}$$

The gas diffusion coefficient is of the order of 10^{-7} m^2/s, i.e., much larger than the liquid diffusion coefficient.

The relative permeability functions depend on their respective saturations as

$$\begin{aligned}&k_{ro}(s_o) \equiv \frac{k_o(s_o)}{k} = \frac{(s_o - s_{or})^2}{(1 - s_{or})^2}\\ &\text{if} \quad s_l \geq s_{or}, \quad 0 \quad \text{if} \quad s_l \leq s_{or},\\ &k_{rg}(s_g) \equiv \frac{k_g(s_g)}{k} = s_g^2.\end{aligned} \tag{2.12}$$

The composition and temperature dependence of the viscosity μ_o is given by Koval (1963)

$$\frac{1}{\mu_o^b} = \frac{\psi_m}{\mu_m^b} + \frac{\psi_l}{\mu_l^b}, \quad \mu_j = \mu_{j0} \exp\left(-\frac{E_j}{RT}\right), \quad (j = m, l), \tag{2.13}$$

where we choose $b = 0.25$; see also Eq. (4.1). In this equation, E_m and E_l are the activation energies for the viscosity of medium and light components in the oleic phase. We use T^m and T^l to denote the activation temperature for the viscosity of medium and light components, which are equal to E_m/R and E_l/R.

By adding up the Eqs. (2.5)–(2.7), the total balance of gas is

$$\partial_t(\varphi \rho_g s_g) + \partial_x(\rho_g u_g) = W_v + (\nu_{gm} - 1)W_{rm} + (\nu_{gl} - 1)W_{rl}. \tag{2.14}$$

The energy balance equation is

$$\partial_t[(C_m + \varphi C_o \rho_o s_o + \varphi C_g \rho_g s_g)\Delta T] + \partial_x[(C_o \rho_o u_o + C_g \rho_g u_g)\Delta T] = \lambda \partial_x^2 T + Q_{rm} W_{rm} + Q_{rl} W_{rl} - Q_v W_v, \tag{2.15}$$

where C_m, C_o, C_g are the heat capacities for the rock matrix, the oleic phase, and gaseous phase, respectively, which are all assumed to be constant and independent of composition. We use λ to denote the effective thermal conductivity. We neglect heat losses, which are usually very small in field applications (however, taking into account heat losses becomes essential for interpreting laboratory experiments). The full system of balance equations includes Eqs. (2.3)–(2.6), (2.14), and (2.15).

The partial pressure of the gaseous hydrocarbon assuming liquid-gas equilibrium is derived using the Clausius-Clapeyron relation and Raoult's law; it can be expressed as

$$Y_l^{eq} P_g = X_l P_{atm} \exp\left[-\frac{Q_v}{R}\left(\frac{1}{T} - \frac{1}{T^{bn}}\right)\right], \tag{2.16}$$

where T^{bn} is the (normal) boiling point of the light component measured at atmospheric pressure P_{atm}. Taking $Y_l^{eq} = 1$ in (2.16), one recovers the actual boiling temperature $T = T^{bl}$ at the elevated gas pressure $P_g > P_{atm}$. We can see that Y_l^{eq} increases with temperature and $Y_l^{eq} \to 1$ as $T \to T^{bl}$. There are better boiling point relations than Clausius-Clapeyron (see Poling et al. (2001)), but this relation is sufficiently accurate for our purposes.

We express the reaction rates for light and medium components by

$$W_{rl} = A_{rl} \varphi X_l \rho_o s_o \left(\frac{P_g Y_\kappa}{P_{atm}}\right)^n \exp\left(-\frac{T_l^{ac}}{T}\right),$$
$$W_{rm} = A_{rm} \varphi X_h \rho_o s_o \left(\frac{P_g Y_\kappa}{P_{atm}}\right)^n \exp\left(-\frac{T_m^{ac}}{T}\right) \tag{2.17}$$

where A_{rl} and A_{rm} are the frequency factors for the oxidation rate of the light and medium components. We use T_l^{ac} and T_m^{ac} to denote the activation temperatures for these oxidation rates. The activation temperature is related to the activation energy E_{act-i} as $T_i^{ac} = E_{act-i}/R$, where $i = l$ (light) and m (medium). Usually $0 < n < 1$, and we use $n = 1$ in our simulation. The vaporization-condensation rate is given by

$$W_v = k_l(Y_l^{eq} - Y_l)\rho_g s_o^{2/3} X_l, \tag{2.18}$$

where we assume that the vaporization rate is proportional to the deviation of the mole fraction of the light component in the gas phase Y_l from its equilibrium value Y_l^{eq}, the surface area $s_o^{2/3}$, the mole fraction of the light component in the liquid phase X_l, and an empirical transfer parameter k_l is equal to 1 which has a dimension of s^{-1} in our simulation. This formulation can be considered to be a consequence of nonequilibrium thermodynamics (see Levenspiel (1999); Prigogine (1962)). The vaporization rate W_v vanishes under the conditions

$$W_v = 0 \text{ when } s_o > 0,\ Y_l = Y_l^{eq} \text{ or } s_o X_l = 0, \tag{2.19}$$

when either there is no liquid light component or it is in thermodynamic equilibrium with the gaseous phase. Note that when condensation occurs in our simulation, the oil saturation is bigger than zero.

2.1 Initial and Boundary Conditions

The initial reservoir conditions are taken as

$$t = 0,\ x \geq 0: \ T = T^{ini},\ s_o = s_o^{ini},\ \psi_m = \psi_m^{ini},\quad Y_l = Y_l^{eq},\quad Y_\kappa = 0,\ P_g = P_{ini}(x). \tag{2.20}$$

These conditions correspond to the reservoir filled by oil and gas (with no oxygen) at given oil saturation, composition, and temperature. It is necessary to specify the initial pressure curve $P_{ini}(x)$ in the domain of interest, i.e., for

$0 \le x \le l$, where l is the length of the system. For simulation purposes the following choice is convenient:

$$P_{ini}(x) = P_{res} + \frac{(l-x)\mu_g u_{inj}}{k_g(s_l^{ini})} \ . \tag{2.21}$$

We use the parameters from Table 1 and l = 100 m.

The injection boundary conditions at $x = 0,\ t \ge 0$ are

$$\begin{aligned} &T = T^{ini}, \quad s_o = 0, \quad \partial_x \psi_m = 0, \quad Y_l = 0, \\ &Y_\kappa = Y_\kappa^{inj}, \quad u = u^{inj}, \end{aligned} \tag{2.22}$$

corresponding to the injection of air at reservoir temperature. The condition $u = u_{inj}$ leads to an injected gas flux of $u_{inj}\rho_g$. It is assumed that there are no gaseous hydrocarbons in the injected gas, i.e., $Y_l = 0$. The production boundary conditions at $x = l$, $t \ge 0$ are

$$\begin{aligned} &\partial_x T = \partial_x s_o = \partial_x \psi_m = \partial_x Y_l = \partial_x Y_\kappa = 0, \\ &P_g = P_{res}, \end{aligned} \tag{2.23}$$

where P_{res} is a constant reservoir pressure. Note that our simulation describes air injection to a reservoir at constant initial temperature, with no use of any additional ignition mechanism.

3. ANALYTICAL SOLUTION FOR ONE-COMPONENT OIL

It is the purpose of this paper to understand the relative importance of vaporization/condensation vs. oxidation, by studying a two-component mixture of volatile and non volatile oil. We first summarize the results of the analytical solution for the one-component system found by Mailybaev et al. (2013) for reasons of easy reference. The analytical solution (Mailybaev et al., 2013) considers the combustion of a one-component light oil (heptane) by medium temperature oxidation (MTO). The numerical results for such oil including molecular diffusion, capillary, and thermal conductivity effects can be found by Khoshnevis Gargar et al. (2014a). Capillary diffusion increases the temperature in the upstream part of the MTO region and decreases the efficiency of oil recovery. However, we showed that for the realistic conditions, the diffusive processes has no significant influence on the behavior of the MTO wave.

Our interest is always in the behavior at large times, when the solution consists of a sequence of waves separated by constant states. It is shown in Fig. 1 and is composed of three waves, i.e., the thermal, the MTO, and the saturation wave. The thermal wave is the slowest wave due to the high heat capacity of the rock. The constant state at the upstream side of the thermal wave is determined by the injection boundary conditions. As shown in Fig. 1, the temperature in the thermal wave changes from $T = T^{ini}$ upstream to some value T^- further downstream. For calculating T^- one can see Eq. (3.26) by Mailybaev et al. (2013). In the case of one-component oil (volatile oil), the MTO region moves with a constant speed v. In this region, all the dependent variables T, s_o, u, Y_l, Y_κ can be expressed in terms of a single traveling coordinate $\xi = x - vt$, i.e., in a frame of reference moving with speed v the profiles are stationary. Mailybaev et al. (2013) use the traveling wave solution to relate quantities at the upstream side (T^-, s_o^-, u^-, Y_l^-, Y_κ^-) to those at the downstream side (T^+, s_o^+, u^+, Y_l^+, Y_κ^+). It turns out that the wave speed v can be obtained from these quantities too. The region upstream the MTO wave contains injected gas with an oxygen fraction $Y_\kappa^{inj} > 0$ and no gaseous hydrocarbon, $Y_l = 0$. The reaction rate w_r vanishes both at the upstream and downstream sides of the

TABLE 1: Values of reservoir parameters for heptane, decane as light, medium pseudo-components

$A_{rl} = A_{rm}$	=	4060 1/s	Q_{rm}	=	400 kJ/mol O_2	u^{inj}	=	8.0×10^{-7} m/s
C_g	=	29 J/mol·K	Q_v	=	31.8 kJ/mol	Y_κ^{inj}	=	0.21
C_m	=	2 MJ/m^3·K	R	=	8.314 J/mol·K	ν_{gm}	=	1.36 (mol/mol)
C_o	=	224 J/mol·K	s_{or}	=	0.1	ν_{om}	=	0.065 (mol/mol)
D_o	=	1×10^{-10} m^2/s	s_l^{ini}	=	0.9	ν_{ol}	=	0.090 (mol/mol)
D_g	=	1×10^{-7} m^2/s	T_l^{ac}	=	7066 K	ν_{gl}	=	1.36 (mol/mol)
k	=	10^{-10} (m^2)	T_m^{ac}	=	10050 K	ρ_L	=	6826 mol/m^3
n	=	1	T^{bn}	=	371 K	φ	=	0.3
P_{res}	=	10^6 Pa	T^{bl}	=	478.5 K	ρ_M	=	5130 mol/m^3
Q_{rl}	=	400 kJ/mol O_2	T^{ini}	=	300 K	λ	=	3 W/m·K

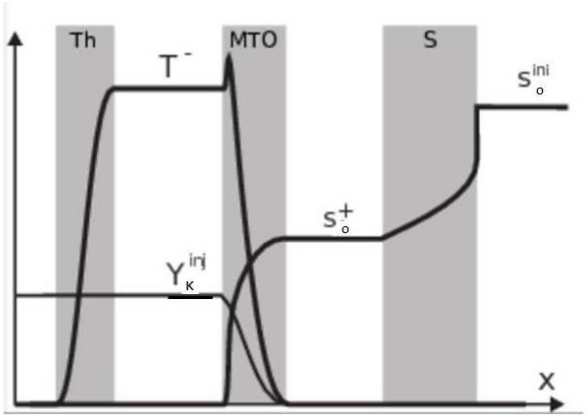

FIG. 1: Wave sequence solutions with the thermal (Th), MTO, and saturation (S) region for light oil (heptane). Indicated are the schematic distributions of the temperature T, oleic saturation s_o and oxygen fraction Y_κ (Mailybaev et al., 2013).

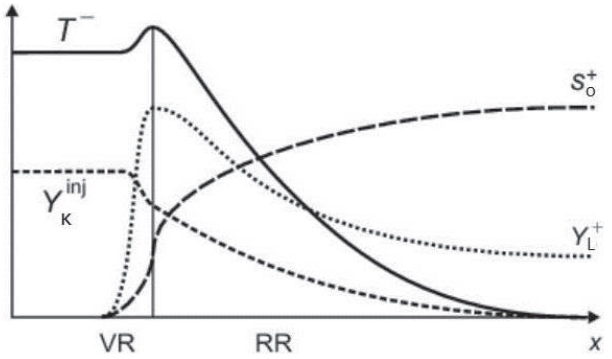

FIG. 2: Schematic graphs of the MTO wave profile in the one-component oil model. Indicated are changes in the temperature T, liquid fuel saturation s_o, oxygen fraction Y_κ, and fuel fraction Y_l in the gas. The thin region VR is dominated by vaporization and the much wider region RR is dominated by the MTO reaction (with slow condensation). The VR is much thinner than the RR, because it is assumed that the vaporization rate is much faster than the reaction rate (Mailybaev et al., 2013).

MTO region; we find the condition $s_o^- = 0$ (no fuel) at the entrance and $Y_\kappa^+ = 0$ (no oxygen) at the production side.

Downstream of the MTO wave there is liquid hydrocarbon with a saturation $s_o^+ > 0$ and temperature $T = T^{ini}$. The equilibrium conditions $W_r = 0$, $W_v = 0$ require $Y_\kappa = 0$ and $Y_l = Y_l^{eq}(T^{ini})$, respectively. Finally, the saturation wave region travels downstream of the MTO wave, see Fig. 1. In this region, the temperature is constant and equal to $T = T^{ini}$. Therefore, we have thermodynamic equilibrium between liquid and vapor heptane, i.e., $Y_l = Y_l^{eq}(T^{ini})$, and there is no net vaporization or condensation. The injected oxygen has been consumed completely in the MTO region. Therefore, we have $Y_\kappa = 0$ in the saturation wave region and no reaction occurs. This region is described by a Buckley-Leverett solution, which uses the standard procedure involving the Welge tangent construction (Welge, 1952). Briefly from upstream to downstream, the Buckley-Leverett solution consists of a rarefaction, a shock, and a constant state; see also (Oleinik, 1959).

We continue to detail the behavior in the MTO region. The mathematical analysis is simplified in an essential way by the physical assumption that the vaporization rate is much faster than the reaction rate. Under this assumption the MTO region is divided into a vaporization region (VR) and a reaction region (RR); see Fig. 2. The VR is very thin. Its width is approximately proportional to the ratio between the reaction and vaporization rates. The surprising feature of MTO is that the thin vaporization region is located upstream of the RR. Here the fraction of gaseous fuel rises from $Y_l = 0$ in the injected gas to the equilibrium value $Y_l = Y_l^{eq}(T)$ at the downstream end of the VR (see Fig. 2). Since this region is very thin and the reaction rate is not large at the prevailing low fuel concentration, the oxygen consumption in the VR is negligible. Downstream of the VR, we have the RR. In the RR, most of the MTO reaction occurs, as well as slow condensation due to temperature decrease in the direction of gas flow. Along the RR, the equilibrium condition $Y_l = Y_l^{eq}(T)$ holds approximately.

4. NUMERICAL MODELING OF TWO-COMPONENT OIL

Let us consider the reservoir parameters given in Table 1. These values correspond to heptane (C_7H_{16}) and decane ($C_{10}H_{22}$) as light (volatile) and medium (non volatile) fractions of the fuel. In Table 1 we used MTO rate parameters compatible with the experimental results by Freitag and Verkoczy (2005). We neglect the capillary effects in the model but the COMSOL software reintroduces numerical diffusion. For the viscosities (cp), we use Sutherland's formula for the gas (air) (Poling et al., 2001) and the Arrhenius model for liquid (heptane and decane) (Poling et al., 2001) given in Pa·s and for T in K as

$$\mu_g = \frac{7.5}{T+120}\left(\frac{T}{291}\right)^{3/2},$$
$$\mu_l = 1.32\times 10^{-2}\exp\left(\frac{1006}{T}\right), \quad (4.1)$$
$$\mu_m = 1.423\times 10^{-2}\exp\left(\frac{1225}{T}\right).$$

We use the quarter power rule for the oil mixture viscosity; see Eq. (2.13).

We utilize a fully implicit numerical solution approach based on finite elements. We formulate and solve the finite element problem with the COMSOL software, which gives numerical results that can be compared to the analytical solution of the one-component model. We apply the mathematical module of COMSOL to introduce the model equations in weak form. We use fifth-order Lagrange elements, which means that the basis functions in this finite element space are polynomials of degree 5. In other words, on each mesh element the solution is a polynomial of degree 5 and the entire solution is a sum of piecewise fifth-order polynomials. The grid size in the numerical simulation is 0.01 m, which is fine enough to capture the multi scale processes and is capable of resolving salient features. Indeed, a spatial resolution of 100/0.01 = 10^4 is enough to resolve qualitatively the fine structure.

4.1 Effect of the Light (Volatile) Component Fraction

As shown in Fig. 3 (left), the numerical solution exhibits a thermal and an MTO region in the same way as did the analytical solution for the one-component system in Fig. 1. In this case the initial volume fraction of the volatile component (C_7H_{16}) is 0.8 in the oil mixture. The saturation region has moved out of sight to the right. For the parameter values used by us, the thermal wave is the slowest wave (it lies between 0 and 25 m in Fig. 3). Therefore, the thermal wave travels in the region of the reservoir from which the light liquid and gaseous hydrocarbons were displaced, i.e., $s_o\psi_l = Y_l = 0$; however, small amounts of medium oil remain behind (between 0 and 10 m), upstream of the MTO wave. The reaction rates W_{rl}, W_{rm} and the vaporization rate W_v are all zero or very small in the thermal wave region. Since there is no reaction in the upstream part of the MTO wave, the oxygen fraction $Y_\kappa = Y_\kappa^{inj}$ is constant. The temperature in the thermal wave changes from the injection value $T = T^{ini}$ upstream to some value T^- in the plateau. The gradual temperature increase is due to the nonzero value of the thermal conductivity in the first term of the right-hand side of Eq. (2.15). The Darcy velocity upstream of the thermal wave is the injection Darcy velocity $u = u_{inj}$ and it increases downstream due to thermal expansion of gas.

The MTO region contains the most interesting wave in our solution, viz., the vaporization/combustion wave; see Fig. 3 (right). Downstream of the MTO region, the temperature is equal to the initial temperature $T = T^{ini}$. This implies the liquid-gas equilibrium $Y_l = Y_l^{eq}(T^{ini})$, and there is neither vaporization nor condensation; see (2.18). No reaction occurs downstream of the MTO region as the oxygen has been consumed completely in the MTO region ($Y_\kappa = 0$); see (2.17).

In summary, when the volatile component represents a large fraction of the oil (in our case $\psi_l^{ini} = 0.8$), vaporization/condensation determines the effectiveness of the combustion process for oil recovery. This effectiveness is more pronounced at lower boiling points. As shown in Fig. 3, vaporization of the light component (heptane) occurs upstream of the region of the reaction (of light and medium oil) in the MTO wave (around 50 m in Fig. 3). Most of the vaporized light component condenses further downstream as the temperature drops down. This fact emphasizes the effectiveness of vaporization/condensation in the displacement of the oil mixture (note the increase of the light component $s_o\psi_l$ as compared to the medium component $s_o\psi_m$ in the upstream side of the MTO wave in Fig. 3). However, not all of the non volatile oil is displaced by the volatile oil, but small amounts remain behind the MTO wave (between 0 and 10 m) because the MTO wave is not initially strong enough to displace the medium oil. This initialization effect causes a slow decrease in the oxygen profile in the first 10 m. The decrease is not visible in Fig. 3 because of the small amounts of fuel and low temperature in that region.

As shown in Fig. 3, the temperature profile is bounded by the boiling temperature (T^{bl} = 478.5 K) of the volatile fraction at elevated pressure. Indeed, one can see that the temperature upstream of the MTO region increases to become close to T^{bl}, as was already conjectured by Mailybaev et al. (2013). The oleic saturation downstream of the MTO region is about 0.67, and from this point, the flow continues with a constant state. The Buckley-Leverett profile may follow further downstream, and this profile passed the right end at the time of Fig. 3.

4.2 Effect of the Medium (Non-Volatile) Component Fraction

The two-component system in which one component evaporates and condenses at low or moderate tempera-

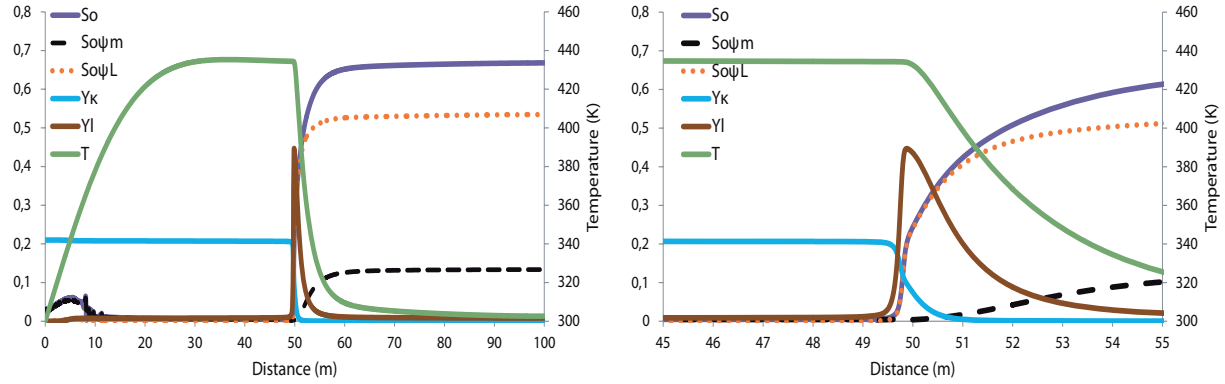

FIG. 3: Simulation for an initial medium component fraction of $\psi_m^{ini} = 0.2$. Wave sequence solution with the thermal and MTO regions. Indicated are the distributions of the temperature T, oleic saturation s_o, oxygen mole fraction Y_κ, gaseous hydrocarbon mole fraction Y_l, light oil concentration $s_o\psi_l$, and medium oil concentration $s_o\psi_m$ at $t = 9.7 \times 10^7$ s in the base case related to Table 1. Note the abrupt decay of the oxygen concentration, the narrow peak of the Y_l concentration, and the rapid decay in temperature representing the MTO region near $x = 50$ m.

tures shows pronounced enhancement of the combustion process effectiveness. Let us study the relative importance of vaporization and combustion in the medium pressure air injection process with different concentrations of the light component. In the base case with medium component volume fraction $\psi_m^{ini} = 0.2$, shown in Fig. 3, vaporization occurs upstream of the MTO wave. Single-component studies (Mailybaev et al., 2013) showed that the combustion front moves considerably faster when vaporization/condensation occurs. In the two-component system $\psi_m^{ini} = 0.2$ shown in Fig. 3, the enhancement of oil recovery by distillation is confirmed.

In Fig. 4, where initial oil is a mixture of light ($\psi_l^{ini} = 0.4$) and medium component ($\psi_m^{ini} = 0.6$), thermal and MTO waves are distinguished. The saturation region has moved out of sight to the right. The general appearance of the solution (Figs. 4 and 3) is preserved even when the fraction of light component decreases to 0.4. The thermal wave travels in the region of the reservoir from which the light liquid and gaseous hydrocarbons were displaced. But a small fraction of medium component remains behind the MTO wave (between 0 and 30 m) because the MTO wave is not initially strong enough to displace the medium oil. This amount (see Fig. 4), however, is considerably larger than the amount in Fig. 3 as a consequence of the presence of three times more non volatile component in the initial mixture (0.6 with respect to 0.2). The presence of left-behind medium oil (initialization effect) in Fig. 4 can explain the smooth temperature increase in the upstream part of the thermal wave (between 10 and 30 m). Since there is some (small) reaction of medium component in the upstream part of the MTO wave, the oxygen fraction $Y_\kappa = Y_\kappa^{inj}$ decreases smoothly but very little before the sharp decline at $x = 63$ m. The temperature in the thermal wave increases from the injection value $T = T^{ini}$ upstream to a peak due to the reaction of oil left behind and then reaches some value T^- in the plateau. The MTO region in Fig. 4 at $x = 63$ m, i.e., the region characterized by the fast decrease in oxygen fraction Y_κ, consists of a region for reaction and another for vaporization. The vaporization region is located upstream of the reaction one. At the upstream side of the MTO region, hydrocarbon evaporates, whereas it condenses at the downstream side (see Y_l in Fig. 4 between 63 and 70 m). The gaseous hydrocarbon profile Y_l has a peak with a finite width.

In Fig. 5, the fraction of the medium component in the initial oil was increased to 0.8. As one can see comparing with Fig. 4, the general appearance of the waves is not preserved. The oil acts more like immobile fuel in the HTO process (Mailybaev et al., 2011b), though it moves slowly through the domain. Vaporization of the light component occurs downstream of the reaction zone (see the profile of Y_l that starts at $x = 40$ m), so that the vaporization is not effective for oil recovery anymore. As shown in Fig. 5, most of the light component is swept away by vaporization, while the medium fraction remains behind and reacts with the oxygen in the injected air (at $x = 5$ m). The two minima in oil saturation s_o in Fig. 5 (at $x = 5$ m and $x = 36$ m) are related to combustion and vaporiza-

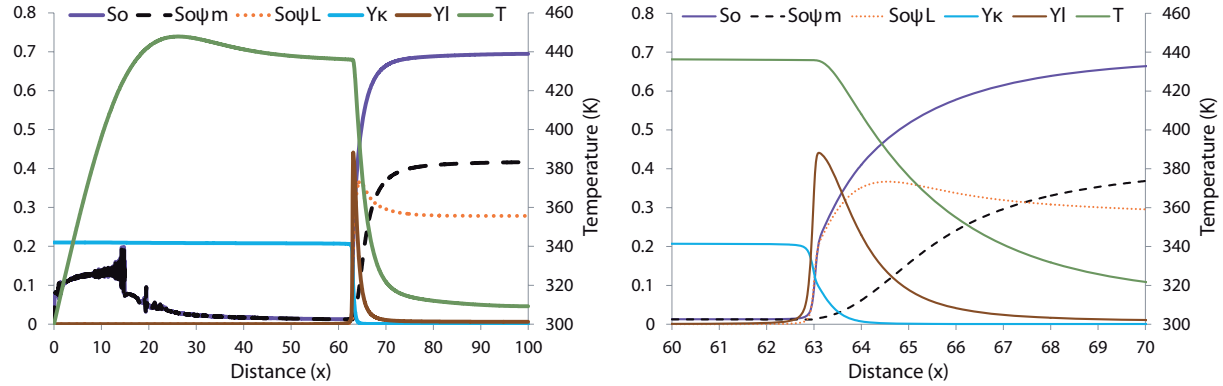

FIG. 4: Simulation for an initial medium component fraction of $\psi_m^{ini} = 0.6$. Wave sequence solution with the thermal and MTO regions. Indicated are the distributions of the temperature T, oleic saturation s_o, oxygen mole fraction Y_κ, gaseous hydrocarbon mole fraction Y_l, light oil concentration $s_o\psi_l$, and medium oil concentration $s_o\psi_m$ at $t = 1.4 \times 10^8$ s in the case related to Table 1. Note the abrupt decay of the oxygen concentration, the narrow peak of the Y_l concentration, and the rapid decay in temperature near $x = 63$ m.

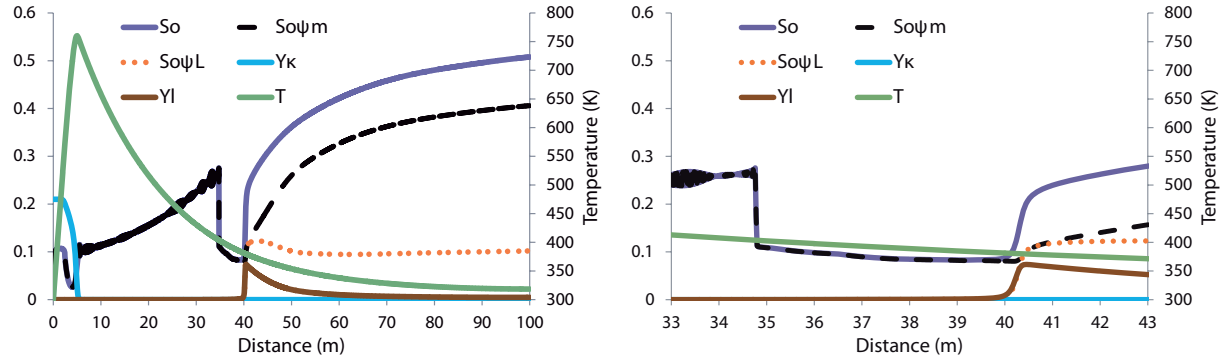

FIG. 5: Simulation for an initial medium component fraction of $\psi_m^{ini} = 0.8$. Indicated are the distributions of the temperature T, oleic saturation s_o, oxygen mole fraction Y_κ, gaseous hydrocarbon mole fraction Y_l, light oil concentration $s_o\psi_l$, and medium oil concentration $s_o\psi_m$ at $t = 2.1 \times 10^8$ s.

tion; we have no correspondence to Fig. 1. In this case, reaction of a large amount of left-behind medium component with oxygen leads to a steep increase in temperature to almost 600°C before the latter decreases to its initial value T^{ini} downstream of the condensation region. Since there is no light component in the reaction zone, the temperature is not bounded by the boiling point of the light component T^{bl}. The gaseous hydrocarbon fraction Y_l increases steeply (at $x = 40$ m in Fig. 5) and then condenses gradually downstream to the equilibrium value at the initial temperature. The slow condensation of hydrocarbon from the gas leads to an increase in the light oil profile in Fig. 5. Note that the behavior near the vaporization region, shown in amplified form in Fig. 5 (right), leads to a large oscillation (a large drop followed by an increase downstream) in non volatile oil component $s_o\psi_m$. The described process has much in common with the HTO description by Mailybaev et al. (2011a,b). However, there are differences such as oscillations in the saturation profile.

We conclude that the MTO wave structure depends drastically on the initial oil composition. When the light component fraction is sufficiently large, the vaporization occurs in the upstream side, leading to effective temperature control and high recovery rate (Figs. 3 and 4). On the contrary, when light oil fraction is low, vaporization region moves to the downstream side of the combustion zone (Fig. 5). This leads to very high temperatures and

slow recovery rate. We should note, however, that our two-component model of MTO is not valid for such high temperatures, because cracking and vaporization of the medium component becomes a relevant part of the process (Mailybaev et al., 2011a,b). Thus, our model is only capable of predicting a qualitative change of the combustion regime, while a specific profile in the case of Fig. 5 must be confirmed using a different model; the latter is a topic for a future research.

4.3 Effect of Air Injection Rate

Now let us study the relative importance of vaporization and combustion in an air injection process under different air injection rates. As shown by Fig. 6, the general appearance of the wave sequences is not preserved for the oil mixture of 0.8 volatile components at a three times higher air injection rate ($u^{inj} = 2.4\times10^{-6}$ m/s). Due to higher injection velocity, a large part of the light component is swept away by the injected gas (see $s_o\psi_l$ in Fig. 6). As shown in Fig. 6 compared to Fig. 3, the amount of evaporated light hydrocarbon (Y_l) decreases significantly with higher injection rates. The left-behind medium component reacts with oxygen (between x = 0–30 m), and releases heat. Because the vaporization is not acting as the dominant recovery method at higher injection rates, the released heat leads to high temperatures, although the initial mixture is light ($\psi_l^{ini} = 0.8$). As seen in Fig. 3 compared to Fig. 6, the downstream liquid saturation stays around the value $s_o^+ \approx 0.65$ for a lower injection rate rather than around $s_o^+ \approx 0.55$ for a higher injection rate. This decrease supports the conclusion that the MTO process is less efficient for light oil recovery under higher injection rates.

Now, we investigate the air injection rate effect on the process effectiveness when the oil mixture is composed of large amounts of non volatile component ($\psi_m^{ini} = 0.8$). As seen in Fig. 7, the recovery process is faster than at a lower injection rate (see Fig. 5). More left-behind oil is combusted and leads to higher temperatures in the domain. For both oil mixtures, Figs. 7 and 6, the oxygen decline is steeper than in the case of low injection rates. The minimum (at x = 2 m) is related to the combustion of the medium component, while the second minimum related to vaporization in Fig. 5 (at x = 36 m) is not seen in the high injection rate profile.

In summary, the increase of injection rate leads to the combustion regime, where reaction occurs upstream of vaporization, resulting in high temperatures and low efficiency of medium oil recovery. As in the previous section, we can rely on our model prediction about the transition to the regime with HTO, but a model with cracking is necessary for an adequate quantitative description at high temperatures.

4.4 Effect of Pressure

This section considers the relative importance of vaporization and combustion in air injection processes under higher pressure in the reservoir. As shown in Fig. 8, the general appearance of the wave sequences is preserved for the oil mixture of 80% volatile components at higher

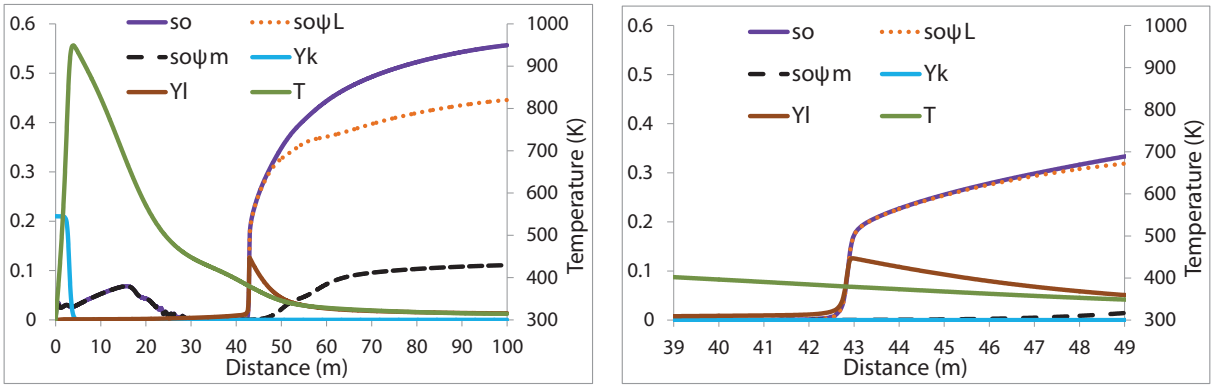

FIG. 6: Simulation for an initial medium component fraction of $\psi_m^{ini} = 0.2$. Indicated are the distributions of the temperature T, liquid saturation s_o, oxygen mole fraction Y_κ, gaseous hydrocarbon mole fraction Y_l, light oil saturation $s_o\psi_l$, and medium oil saturation $s_o\psi_m$ at $t = 4.6\times10^7$ s in the case related to Table 1 but with a three times higher air injection rate.

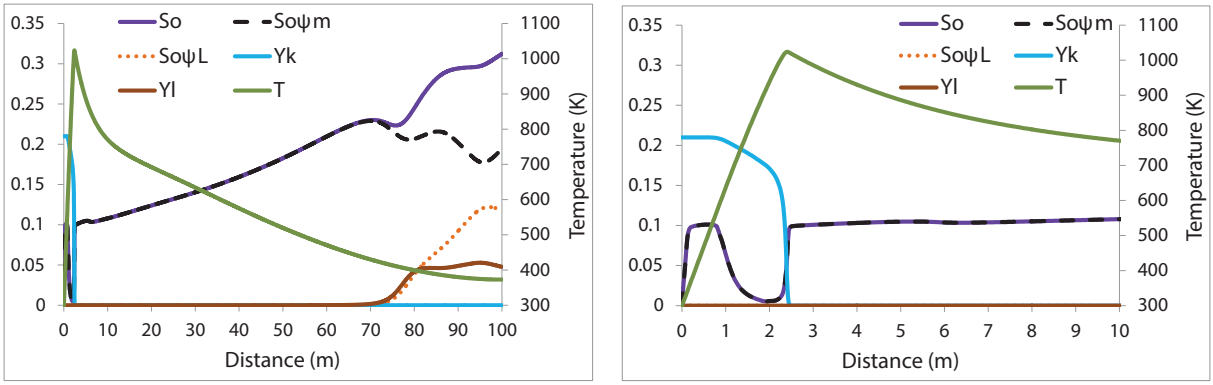

FIG. 7: Simulation for an initial medium component fraction of $\psi_m^{ini} = 0.8$. Indicated are the distributions of the temperature T, liquid saturation s_o, oxygen mole fraction Y_κ, gaseous hydrocarbon mole fraction Y_l, light oil saturation $s_o\psi_l$, and medium oil saturation $s_o\psi_m$ at $t = 1.26 \times 10^8$ s in the case related to Table 1 but with a three times higher air injection rate.

pressure (P_{res} = 30 bars). The thermal, MTO, and saturation wave velocities get higher when the reservoir pressure increases from 10 bars (see Fig. 3) to 30 bars (see Fig. 8). We see that the downstream liquid saturation stays around the value $s_o^+ \approx 0.7$ for both pressures, albeit this value slowly increases with increasing pressure, in agreement with the analytical result based on a single pseudo-component oil model (Mailybaev et al., 2013). Pressure increase leads to an increase of temperature as well as an increase of the MTO wave speed relative to the injection speed. When the oil mixture is light, the temperature in the thermal wave is still bounded by the boiling temperature of the volatile oil at elevated pressure. The width of the reaction region (RR) evaluated by the decline of oxygen concentration is of the order of 1.5 m in the lower pressure model shown in Fig. 3, while the width in the higher pressure solution (Fig. 8) is of the order of 40 cm. Higher pressure leads to a higher reaction rate [see Eq. (2.17)], and hence a rapid decline in oxygen fraction. It seems that the vaporization is slightly less effective in the high pressure regime (see Y_l in Fig. 8) than in the moderate pressure regime.

5. CONCLUSIONS

Oil recovery by air injection is a promising method to improve recovery of light/medium oil from low permeability reservoirs; it can be modeled as a medium temperature oxidation (MTO) process. We proposed a model considering vaporization, condensation, and reaction with

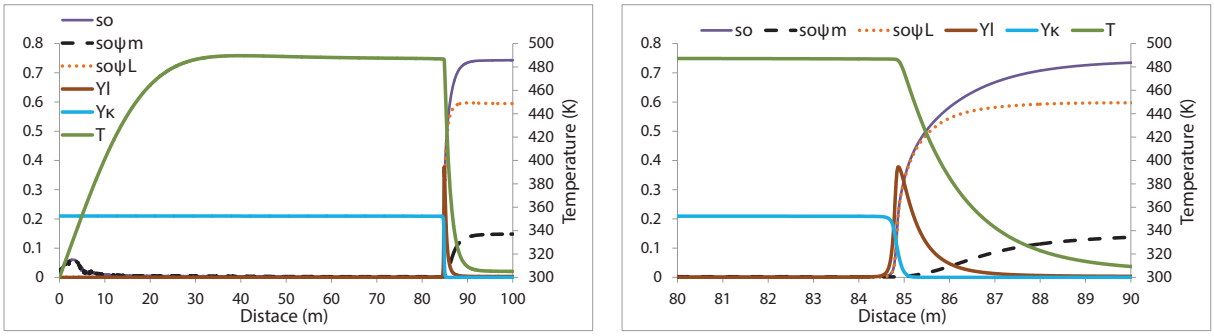

FIG. 8: Simulation for an initial medium component fraction of $\psi_m^{ini} = 0.2$; wave sequence solution with the thermal and MTO regions. Indicated are the distributions of the temperature T, liquid saturation s_o, oxygen mole fraction Y_κ, gaseous hydrocarbon mole fraction Y_l, light oil saturation $s_o\psi_l$, and medium oil saturation $s_o\psi_m$ at $t = 8 \times 10^7$ s in the case related to Table 1 but with a higher pressure, P_{res} = 30 bars.

oxygen. It includes three gaseous components (oxygen, gaseous hydrocarbon, and remaining gas) and two components (volatile and non volatile) in the oil phase, and consists of the mass and energy balance equations. The MTO combustion completely displaces the oil at the expense of small amounts of burned oil. A mathematical model was proposed to study the effect of oil composition, air injection rate, and pressure on the role of vaporization/condensation and combustion during oil recovery by MTO combustion in porous media.

We used a high-order finite element software package (COMSOL) to obtain numerical solutions for different mixtures of volatile and non volatile oil. The character of the MTO wave changes by altering the composition of the oil. Generally the solution consists of three waves, i.e., a thermal wave, an MTO wave, and a saturation wave separated by constant state regions, while the order between vaporization and oxidation in the MTO wave changes for different sets of conditions. For a predominantly light oil mixture, vaporization occurs upstream of the combustion process, a fact that is also confirmed by previously obtained analytical and numerical solutions for one-component volatile oil (Khoshnevis Gargar et al., 2014a; Mailybaev et al., 2013). The combustion front velocity is high as less oil remains behind in the combustion zone. For oil with more non volatile component (0.8 in volume fraction), the vaporization moves to the downstream side of the combustion zone in the MTO wave. As more oil stays behind in the combustion zone, the velocity of the combustion zone is slower, albeit with much higher temperatures. Due to high temperatures, we conjecture a transition to the HTO combustion mechanism in this case, which should be confirmed using a more elaborate model.

The simulations show that there is a bifurcation point, determined by the fraction of the medium component, where the character of the combustion process changes from a vaporization-dominated to a combustion-dominated process. In a vaporization-dominated process less oil stays behind in the reservoir. Numerical calculations make it possible to establish a range of parameters for the bifurcation point, where the character of the combustion changes from a predominance of vaporization to a predominance of combustion. Finally, the MTO wave is less efficient for light oil recovery under higher air injection rates, but the recovery is faster at higher pressure.

ACKNOWLEDGMENTS

This research was carried out within the context of the ISAPP Knowledge Centre. ISAPP (Integrated Systems Approach to Petroleum Production) is a joint project of the Netherlands Organization of Applied Scientific Research TNO, Shell International Exploration and Production, and Delft University of Technology. The paper was also supported by grants of PRH32 (ANP 731948/2010, Petrobras 6000.0069459.11.4), FAPERJ (E-26/102.965/2011, E-26/111.416/2010, E-26/110.658/2012, E-26/110.237/2012, E-26/111.369/2012) and CNPq (301564/2009-4, 477907/2011-3, 305519/2012-3, 402299/2012-4, 470635/2012-6) and Capes/Nuffic 024/2011. The authors thank TU Delft and IMPA for providing the opportunity for this work.

REFERENCES

Abou-Kassem, J. H., Farouq Ali, S. M., and Ferrer, J., Appraisal of steamflood models, *Rev. Tec. Ing.*, vol. **9**, pp. 45–58, 1986.

Adegbesan, K., Donnelly, J., Moore, R., Bennion, D., Low-temperature oxidation kinetic parameters for in-situ combustion numerical simulation, *SPE Reservoir Eng.*, vol. **2**, pp. 573–582, 1987.

Akin, S., Kok, M., Bagci, S., and Karacan, O., Oxidation of heavy oil and their SARa fractions: Its role in modeling in-situ combustion, In *Proc. of SPE Annual Technical Conference*, Dallas TX, SPE 63230, 2000.

Akkutlu, I., Yortsos, Y., Steady-state propagation of in-situ combustion fronts with sequential reactions, In *Proc. of SPE International Petroleum Conference in Mexico*, 2004.

Akkutlu, I., Yortsos, Y., and Lu, C., Insights into in-situ combustion by analytical and pore-network modeling, In *Proc. of SPE International Thermal Operations and Heavy Oil Symposium*, 2005.

Alexander, J., Martin, W. L., and Dew, J., Factors affecting fuel availability and composition during in situ combustion, *J. Pet. Technol.*, vol. **14**, pp. 1154–1164, 1962.

Bamford, C. and Tipper, C., *Comprehensive Chemical Kinetics*, *vol. **17**, Gas-phase Combustion*, Amsterdam: Elsevier, 1977.

Belgrave, J. and Moore, R., A model for improved analysis of in-situ combustion tube tests, *J. Pet. Sci. Eng.*, vol. **8**, pp. 75–88, 1992.

Bird, R., Stewart, W., and Lightfoot, E., *Transport Phenomena*, New York: Wiley, 2002.

Bruining, J., Mailybaev, A., and Marchesin, D., Filtration combustion in wet porous medium, *SIAM J. Appl. Math.*, vol. **70**, pp. 1157–1177, 2009.

Castanier, L. and Brigham, W., Modifying in-situ combustion with metallic additives, *In Situ*, vol. **21**, pp. 27–45, 1997.

Castanier, L. and Brigham, W., Upgrading of crude oil via in situ combustion, *J. Pet. Sci. Eng.*, vol. **39**, pp. 125–136, 2003.

Crookston, R., Culham, W., and Chen, W., A numerical simula-

tion model for thermal recovery processes, *Soc. Pet. Eng. J.*, vol. **19**, pp. 37–58, 1979.

De Zwart, A., van Batenburg, D., Blom, C., Tsolakidis, A., Glandt, C., and Boerrigter, P., The modeling challenge of high pressure air injection, In *Proc. of SPE/DOE Symposium on Improved Oil Recovery*, Tulsa, OK, 2008.

Fassihi, M., Brigham, W., and Ramey Jr, H., Reaction kinetics of in-situ combustion: Part 1—observations, *SPE J.*, vol. **24**, pp. 399–407, 1984.

Fassihi, M., Yannimaras, D., and Kumar, V., Estimation of recovery factor in light-oil air-injection projects, *SPE Reservoir Eng.*, vol. **12**, pp. 173–178, 1997.

Fisher, E., Pitz, W., Curran, H., and Westbrook, C., Detailed chemical kinetic mechanisms for combustion of oxygenated fuels, *Proc. of Combustion Inst.*, vol. **28**, pp. 1579–1586, 2000.

Freitag, N. and Verkoczy, B., Low-temperature oxidation of oils in terms of SARA fractions: Why simple reaction models don't work, *J. Can. Pet. Technol.*, vol. **44**, pp. 54–61, 2005.

Germain, P. and Geyelin, J., Air injection into a light oil reservoir: The Horse Creek project, In *Proc. of Middle East Oil Show and Conference*, Bahrain, Paper SPE-37782-MS, 1997.

Gerritsen, M., Kovscek, A., Castanier, L., Nilsson, J., Younis, R., and He, B., Experimental investigation and high resolution simulator of in-situ combustion processes; 1. simulator design and improved combustion with metallic additives, *SPE International Thermal Operations and Heavy Oil Symposium and Western Regional Meeting*, 2004.

Gillham, T., Cerveny, B., Fornea, M., and Bassiouni, D., Low cost ior: An update on the w. hackberry air injection project, *Paper SPE-39642 presented at the SPE/DOE Improved Oil Recovery Symposium*, Tulsa, Oklahoma, April, 19–22, 1998.

Gottfried, B., A mathematical model of thermal oil recovery in linear systems, *Soc. Pet. Eng. J.*, vol. **5**, pp. 196–210, 1965.

Greaves, M., Ren, S., Rathbone, R., Fishlock, T., and Ireland, R., Improved residual light oil recovery by air injection (LTO process), *J. Can. Pet. Technol.*, vol. **39**, pp. 57–61, 2000a.

Greaves, M., Young, T., El-Usta, S., Rathbone, R., Ren, S., and Xia, T., Air injection into light and medium heavy oil reservoirs: Combustion tube studies on west of Shetlands Clair oil and light Australian oil, *Chem. Eng. Res. Des.*, vol. **78**, pp. 721–730, 2000b.

Gutierrez, D., Skoreyko, F., Moore, R., Mehta, S., and Ursenbach, M., The challenge of predicting field performance of air injection projects based on laboratory and numerical modelling, *J. Can. Pet. Technol.*, vol. **48**, pp. 23–33, 2009.

Gutierrez, D., Taylor, A., Kumar, V., Ursenbach, M., Moore, R., and Mehta, S., Recovery factors in high-pressure air injection projects revisited, *SPE Reservoir Eval. Eng.*, vol. **11**, pp. 1097–1106, 2008.

Hardy, W., Fletcher, P., Shepard, J., Dittman, E., and Zadow, D., In-situ combustion in a thin reservoir containing high-gravity oil, *J. Petr. Technol.*, vol. **24**, pp. 199–208, 1972.

Helfferich, F., *Kinetics of Multistep Reactions*, Amsterdam, Elsevier, 2004.

Huffman, G., Benton, J., El-Messidi, A., and Riley, K., Pressure maintenance by in-situ combustion West Heidelberg unit, Jasper County Mississippi, *J. Petr. Technol.*, vol. **35**, no. 10, SPE-10247-PA, 1983.

Khorsandi Kouhanestani, S., Bozorgmehry Boozarjomehry, R., and Pishvaie, M., Fully implicit compositional thermal simulator using rigorous multiphase calculations, *Sci. Iran.*, vol. **18**, pp. 509–517, 2011.

Khoshnevis Gargar, N., Achterbergh, N., Rudolph-Flöter, S., and Bruining, H., In-situ oil combustion: Processes perpendicular to the main gas flow direction, In *Proc. of SPE Annual Technical Conference and Exhibition*, Florence, Italy, SPE Paper 134655-MS, 2010.

Khoshnevis Gargar, N., Mailybaev, A., Bruining, J., and Marchesin, D., Diffusive effects on recovery of light oil by medium temperature oxidation, *Transp. Porous Media*, vol. **105**, no. 1, pp. 191–209, 2014a.

Khoshnevis Gargar, N., Mailybaev, A., Marchesin, D., and Bruining, J., Recovery of light oil by air injection at medium temperature: Experiments, *J. Pet. Sci. Eng.*, (submitted), 2014b.

Kok, M. and Karacan, C., Behavior and effect of SARA fractions of oil during combustion, *SPE Reservoir Eval. Eng.*, vol. **3**, pp. 380–385, 2000.

Koval, E., A method for predicting the performance of unstable miscible displacement in heterogeneous media, *Soc. Pet. Eng. J.*, vol. **3**, pp. 145–154, 1963.

Kumar, M., Simulation of laboratory in-situ combustion data and effect of process variations, *SPE Symp. Reservoir Simul.*, 1987.

Kumar, V., Gutierrez, D., Thies, B., and Cantrell, C., Thirty years of successful high-pressure air injection: Performance evaluation of Buffalo Field, South Dakota, In *Proc. of SPE Annual Technical Conference and Exhibition*, SPE paper 133494-MS, 2010.

Levenspiel, O., *Chemical Reaction Engineering*, New York, John Wiley & Sons, 1999.

Li, J., Mehta, S., Moore, R., Ursenbach, M., Zalewski, E., Ferguson, H., and Okazawa, N., Oxidation and ignition behaviour of saturated hydrocarbon samples with crude oils using TG/DTG and DTA thermal analysis techniques, *J. Can. Pet. Technol.*, vol. **43**, pp. 45–51, 2004.

Lin, C., Chen, W., Lee, S., and Culham, W., Numerical simulation of combustion tube experiments and the associated kinetics of in-situ combustion processes, *SPE J.*, vol. **24**, pp. 657–666, 1984.

Lin, C., Chen, W., and Culham, W., New kinetic models for thermal cracking of crude oils in in-situ combustion processes, *SPE Reservoir Eng.*, vol. **2**, pp. 54–66, 1987.

Mailybaev, A., Bruining, J., and Marchesin, D., Analysis of in situ combustion of oil with pyrolysis and vaporization, *Combust. Flame*, vol. **158**, pp. 1097–1108, 2011a.

Mailybaev, A., Bruining, J., and Marchesin, D., Analytical formulas for in-situ combustion, *SPE J.*, vol. **16**, pp. 513–523, 2011b.

Mailybaev, A., Marchesin, D., and Bruining, J., Recovery of light oil by medium temperature oxidation, *Transp. Porous Media*, vol. **97**, pp. 317–343, 2013.

Montes, A., Gutierrez, D., Moore, R., Mehta, S., and Ursenbach, M., Is high-pressure air injection (hpai) simply a fluegas flood?, *J. Canadian Petrol. Technol.*, vol. **49**, pp. 56–63, 2010.

Oleinik, O., Construction of a generalized solution of the Cauchy problem for a quasi-linear equation of first order by the introduction of vanishing viscosity, *Usp. Mat. Nauk*, vol. **14**, pp. 159–164, 1959.

Parrish, D. R., Pollock, C. B., and Craig Jr, F., Evaluation of COFCAW as a tertiary recovery method, Sloss Field, Nebraska, *J. Petrol. Technol.*, vol. **26**, pp. 676–686, 1974a.

Parrish, D. R., Pollock, C. B., Ness, N., and Craig Jr, F., A tertiary COFCAW pilot test in the Sloss Field, Nebraska, *J. Petrol. Technol.*, vol. **26**, pp. 667–675, 1974b.

Poling, B., Prausnitz, J., John Paul, O., and Reid, R., *The Properties of Gases and Liquids*, New York, McGraw-Hill, 2001.

Prigogine, I., *Introduction to Non-Equilibrium Thermodynamics*, New York, John Wiley & Sons, NY, 1962.

Schott, G., Kinetic studies of hydroxyl radicals in shock waves. III. The OH concentration maximum in the hydrogen-oxygen reaction, *J. Chem. Phys.*, vol. **32**, pp. 710–716, 1960.

Wahle, C., Matkowsky, B., and Aldushin, A., Effects of gas-solid nonequilibrium in filtration combustion, *Combust. Sci. Technol.*, vol. **175**, pp. 1389–1499, 2003.

Welge, H., A simplified method for computing oil recovery by gas or water drive, *Trans. AIME*, vol. **195**, pp. 91–98, 1952.

Xu, Z., Jianyi, L., Liangtian, S., Shilun, L., and Weihua, L., Research on the mechanisms of enhancing recovery of light-oil reservoir by air-injected low-temperature oxidation technique, *Natural Gas Ind.*, vol. **24**, pp. 78–80, 2004.

Yortsos, Y. and Akkutlu, I., *Investigation of Multiscale and Multiphase Flow, Transport and Reaction in Heavy Oil Recovery Processes*, U.S. Department of Energy, National Petroleum Technology Office, National Energy Technology Laboratory, 2001.

Youngren, G. K., Development and application of an in-situ combustion reservoir simulator, *Soc. Petr. Eng. J.*, vol. **20**, pp. 39–51, 1980.